

## Elementary Steps in Ziegler-Natta Catalysis\*

GERHARD FINK, R. ROTTLE, D. SCHNELL, and W. ZOLLER, *Institut für Technische Chemie der Technischen Universität München, D 8 München 2, Germany*

### Synopsis

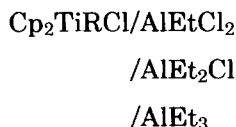
This paper is a short review of our recent advances in Ziegler-Natta catalyst systems of the type  $(C_5H_5)_2TiRCl/AlEt_nCl_m$ . These are, for instance, the electronic changes after complex formation, the parallel reactions of the alkyl and chain transfer between both the Ti centers of two complexes and the Ti center and an Al center of two complexes; furthermore, the alkyl, chain, and chlorine transfers between these complexes and dimer Al-alkyl, the time which the insertion step of one ethylene requires, and the mathematical calculation of the kinetics of the polyreaction.

### INTRODUCTION

The objective of our investigations is the quantitative exploration and formulation of all elementary reactions of soluble Ziegler-Natta catalysts down to the elementary steps in catalytic action. Only within this wide scope is it possible to resolve the inquiry into the nature and structure of the polymerization active species of these complex and very dynamical systems.

This paper restricts itself to a few themes laying a particular stress on two new aspects. These are the great number of elementary reactions between the catalyst components and the enormous dynamic behavior of these soluble systems so far investigated by us. These two new aspects also result in a new point of view about the possible structure of the active species.

Our primary object is the measurement of exact and real experimental data; hence, we restricted ourselves intentionally to one group of soluble systems and tried different methods. This paper, therefore, deals with the catalyst reactions and with the polyinsertion of ethylene with systems of the type bis(cyclopentadienyl)titanium(IV) monochloride monoalkyl and aluminum-alkyl chlorides:



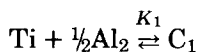
with R = methyl, ethyl, and higher alkyl.

\* Presented at the Polymerization and Polycondensation Processes Symposium, 169th National Meeting of the American Chemical Society, Philadelphia, Pennsylvania, April 6-11, 1975. This paper was not received in time to appear in the proceedings published as *Applied Polymer Symposium No. 26*.

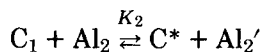
## MATHEMATICAL CALCULATION OF KINETICS OF POLYREACTION

This first theme demonstrates in the system  $\text{Cp}_2\text{Ti-propyl-Cl/AlEtCl}_2$  (as example) by mathematical modeling the quantitative calculation and description of the reaction scheme of the polyreaction; this scheme was postulated according to our extensive kinetical analysis:<sup>1</sup>

Primary equilibrium



Second equilibrium



with  $\text{Ti} = \text{Cp}_2\text{Ti-propyl-Cl}$  free in solution,  $\text{Al}_2 = (\text{AlEtCl}_2)_2$  free in solution,  $\text{C}_1 = \text{Al/Ti} = 1:1$  inactive primary complex,  $\text{C}^* = \text{Al/Ti} = 1:1$  active species, and  $\text{Al}_2' =$  dimeric aluminum species of unknown nature.

As Reichert<sup>2,3</sup> showed for the first time, the polymerization active species is formed in an equilibrium following the formation of the primary complex with the Al component still being a part of the process. Hence, the propagation process of a growing species is an intermittent process which results in a particular<sup>4</sup> molecular weight distribution of the formed polymer.

According to the fact stated above and to the location of the two successive equilibria, the rate law of the polyreaction,

$$v_p = k_p \cdot [\text{C}^*] \cdot [\text{M}]$$

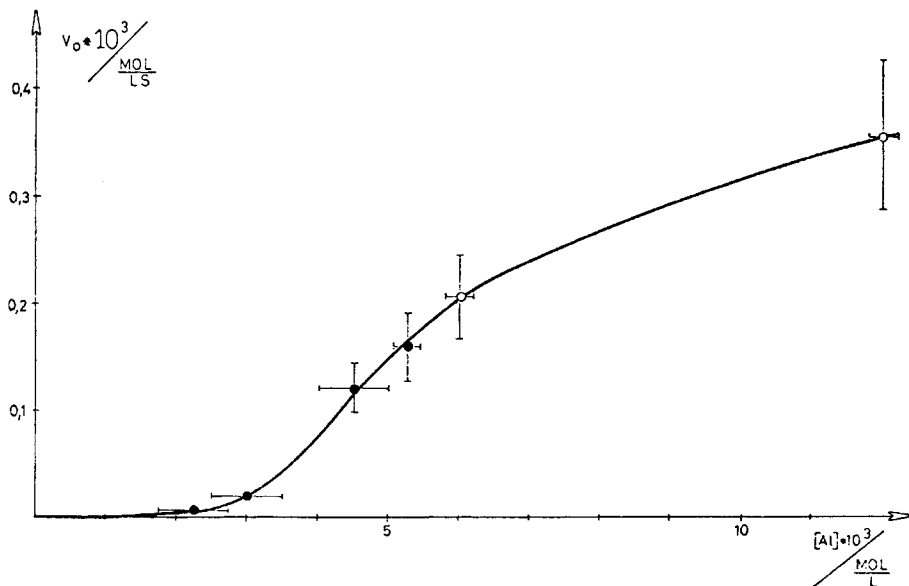


Fig. 1. Initial part of the Al isotherm system  $\text{Cp}_2\text{Ti-propyl-Cl/AlEtCl}_2$ .  $[\text{Ti}] = 3 \text{ mmole/l.}$ ;  $[\text{C}_2\text{H}_4] = 0.089 \text{ mole/l.}$ ;  $T = 10^\circ\text{C.}$

with

$$[C^*] = f(K_1, K_2, Ti_0, Al_0)$$

has to contain a multiplicative term of the two equilibria constants, i.e., the dependence of the polymerization velocity  $v_p$  on the charged Al concentration  $Al_0$  (that is, the Al isotherm) has to show a sigmoidal curve character in the initial part. Figure 1 shows the experimental evidence by means of measurements in a batch reactor. The polymerization velocity is determined here by consumption of ethylene by means of a very sensitive method.<sup>1</sup>

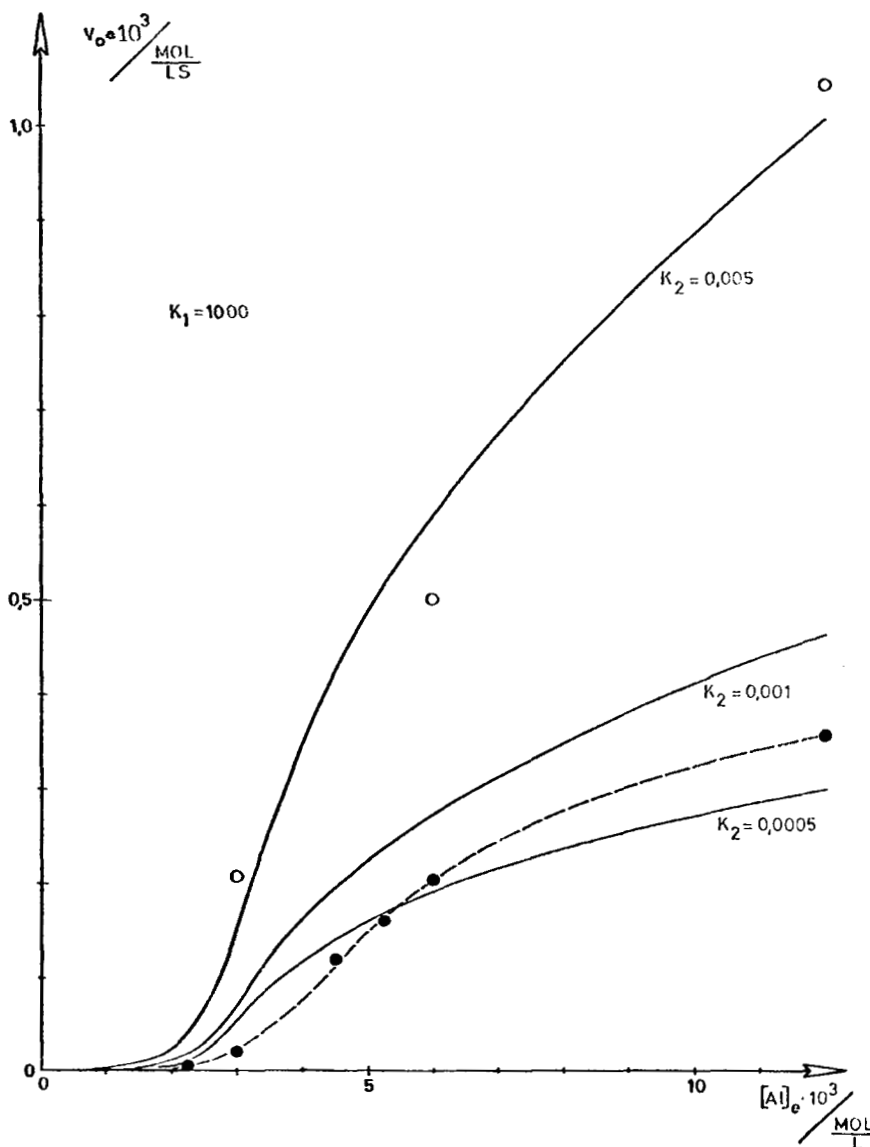


Fig. 2. Comparison of experimental and calculated Al isotherms according to  $V_p = k_p [C^*][M]$ ;  $[M] = [C_2H_4] = 0.089$  mole/l.;  $[C^*]$  from computation (see text); for  $k_p$  determination see text; (●) measurements in batch reactor; (O) measurements in plug flow reactor.

In order to compute the curve in Figure 1, we have four destination equations, these are:

$$\frac{[C_1]}{[Ti] \cdot [Al_2]^{0.5}} = K_1 \quad (1)$$

$$\frac{[C^*]^2}{[C_1] \cdot [Al_2]} = K_2 \quad (2)$$

$$[Ti]_0 = [Ti] + [C_1] + [C^*] \quad (3)$$

$$[Al]_0 = 2[Al_2] + [C_1] + [C^*] + 2[Al_2'] \quad (4a)$$

Because  $[C^*] = [Al_2']$ , (4a) is simplified to

$$[Al]_0 = 2[Al_2] + [C_1] + 3[C^*] \quad (4b)$$

There remain, however, six unknown quantities:  $[C^*]$ ,  $[C_1]$ ,  $[Ti]$  free in solution,  $[Al_2]$  free in solution, and the two equilibrium constants  $K_1$  and  $K_2$ .

We resolved this system of equations iteratively by means of a computer varying  $K_1$  and  $K_2$  in a broad interval without any presupposition, for each single pair of constants followed the variation of the Al concentration again. Part of the results is demonstrated in Figure 2, which shows the comparison of calculated with experimental Al isotherms. The lower points on the dashed line are measurements in the batch reactor, whereas the upper points are measurements by means of an entirely different method, namely, "the oligomer kinetics in a plug flow reactor"<sup>5</sup> (see below). As visible in the diagram, the limiting calculated curves lead to values of the equilibrium constants of  $K_1 = 1000$  and  $K_2 = 0.001$  to  $0.005$ . We can summarize this result thus: we now know exactly the initial concentration of the active species in dependence on the ratio Al/Ti.

### KINETIC DETAIL BY MEANS OF A PLUG FLOW REACTOR

This subject deals with the application of a plug flow reactor in connection with quantitative gel permeation chromatography analysis. By this method, unequivocal kinetic detail is accessible, particularly during the formation of the oligomers.<sup>5</sup> An alkyl transfer between the Al and the Ti component and the influence of the chain length of the starting Ti component on the propagation rate have thus been detected. For example, Figure 3 shows the oligomer distribution in dependence on the alkyl chain length of the charged Ti component (time of direct contact here was 0.29 sec, and the Al/Ti ratio, 10). The appearance of a butane peak with a charged Ti-propyl, Ti-pentyl, Ti-hexyl, respectively, is due to a transfer reaction within which the corresponding Ti-alkyl group is exchanged for an ethyl group of the Al component. The originated Ti-ethyl compound could then generate Ti-butane by ethylene insertion.

Quantitatively separated distributions of this kind were evaluated according to two points of view: (i) The experimental distribution could be described precisely by means of a model computation based again on the concept of the two successive equilibria (paper in preparation); the comparison of experimental and calculated distributions led additionally to an exact cal-

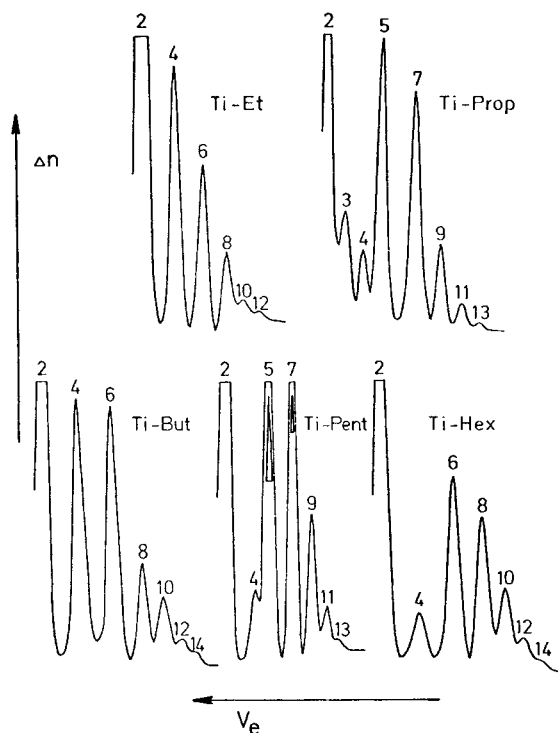


Fig. 3. Gel chromatographic oligomer distributions in dependence on the alkyl chain length of the charged Ti component. Numbers on top of the peaks represent the C number of the formed alkanes;  $[\text{Cp}_2\text{TiRCl}] = 10$  mmoles/l.;  $[\text{AlEtCl}_2] = 100$  mmoles/l.;  $[\text{C}_2\text{H}_4] = 0.22$  mole/l.;  $T = 10^\circ\text{C}$ ; contact time (plug flow reactor) = 0.29 sec.

culuation of homogeneous  $k_p$ . (ii) The graphic integration of the elution curves yields ethylene consumption as a function of the residence time and thus produces a middle polymerization rate, measured, however, by very short and precise reaction times.

Thus, in Figure 4, such a  $\bar{v}_p$  is plotted versus the alkyl-C number of the starting Ti component: the strong dependence on the chain length is obvious. The effect decreases the longer the chain.

The determination of the reaction order of the above-mentioned alkyl transfer reaction concerning the aluminum component is demonstrated in Figure 5. According to the plot,  $\log V_{\bar{u}}$  versus  $\log (\text{Al}_0 - \text{Ti}_0)/2$  results in a first-order obeying dimeric  $[\text{AlEtCl}_2]$  free in solution. The diagram contains another detail: this transfer reaction shows no dependence on the chain length of the Ti component. The activation energy of this transfer reaction was determined to be about 14 kcal/mole.

Finally, the right-hand side ( $\text{C}_6$ ,  $\text{C}_8$ ) of the gel chromatogram in Figure 6 demonstrates that in the case of Ti-hexyl within a residence time of 0.095 sec, only one ethylene molecule has been inserted. (The run in Fig. 6 was carried out with a 1:1 mixture of Ti-ethyl and Ti-hexyl originally in order to emphasize the dependence on the chain length; as is obvious, more butane originated from Ti-ethyl than octane from Ti-hexyl.)

The appearance of octane only with charged Ti-hexyl shows that in this experiment for the first time it was possible to measure the time of one inser-

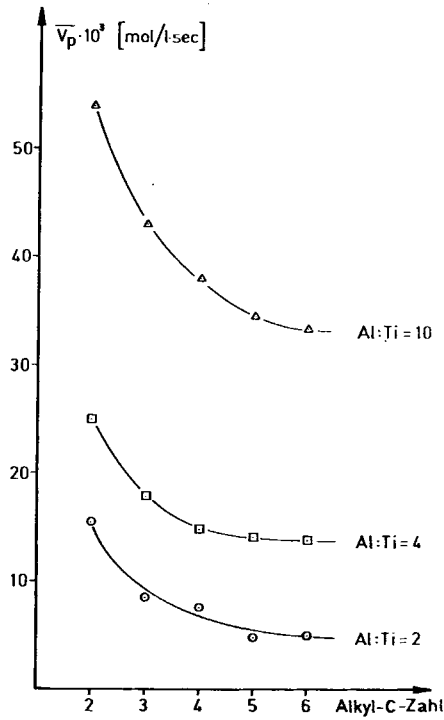


Fig. 4. Plot of  $\bar{V}_p$  (from graphic integration of GPC elution curves) vs. chain length of the starting Ti component.  $[\text{Cp}_2\text{TiRCl}] = 10$  mmol/l;  $[\text{AlEtCl}_2] = 20$  mmol/l, 40 mmol/l, 100 mmol/l;  $[\text{C}_2\text{H}_4] = 0.22$  mole/l;  $T = 10^\circ\text{C}$ ; contact time (plug flow reactor) = 0.29 sec.

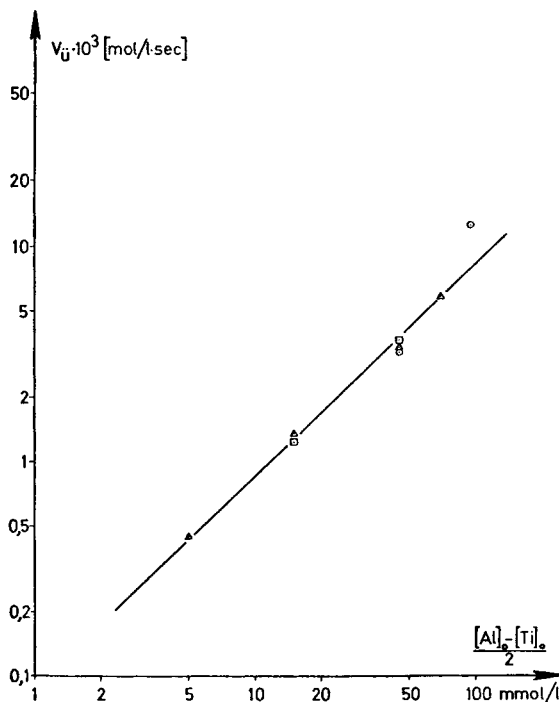


Fig. 5. Determination of the reaction order of the Al-alkyl transfer reaction (see text); system  $\text{Cp}_2\text{TiRCl}/\text{AlEtCl}_2$ .  $[\text{Cp}_2\text{TiRCl}] = 10$  mmol/l; (○) Ti-propyl; (+) Ti-pentyl; (●) Ti-hexyl;  $[\text{C}_2\text{H}_4] = 0.22$  mole/l;  $T = 10^\circ\text{C}$ ; contact time (plug flow reactor) = 0.29 sec.

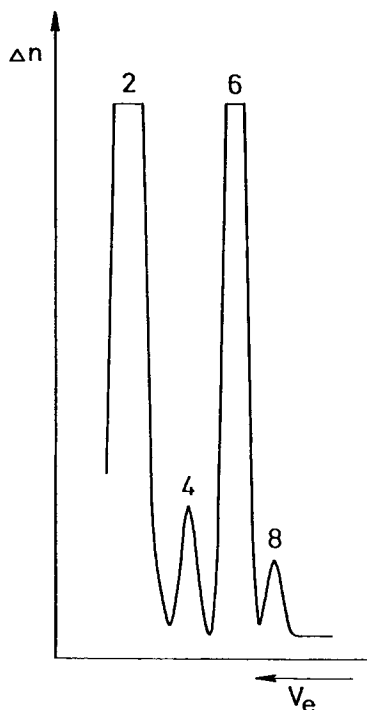


Fig. 6. Oligomer distribution with a charged mixture of  $\text{Cp}_2\text{Ti-ethyl-Cl}$  and  $\text{Cp}_2\text{Ti-hexyl-Cl}$ . Contact time (plug flow reactor) = 0.095 sec;  $[\text{Cp}_2\text{Ti-ethyl-Cl}] = 5$  mmoles/l.;  $[\text{Cp}_2\text{Ti-hexyl-Cl}] = 5$  mmoles/l.;  $[\text{AlEtCl}_2] = 20$  mmoles/l.;  $[\text{C}_2\text{H}_4] = 0.22$  mole/l.;  $T = 10^\circ\text{C}$ .

tion step: it requires 95 msec in the case of Ti-hexyl. Taking into account the dependence on the chain length, the insertion in a Ti-ethyl bond requires about 30 msec in toluene at a temperature of  $10^\circ\text{C}$  and an ethylene concentration of 0.22 mole/l. These values lead directly to  $k_{p \text{ hexyl}} = 47$  l./mole-sec and  $k_{p \text{ ethyl}} = 146$  l./mole-sec (for  $10^\circ\text{C}$  in toluene).

### KINETIC AND MECHANISTIC DETAIL BY MEANS OF $^{13}\text{C}$ -NMR SPECTROSCOPY

This third subject deals with dynamic  $^{13}\text{C}$ -NMR spectroscopy used for the first time in soluble Ziegler catalyst systems. This method turns out to be a molecular surveyor, and these first results let us expect further direct insight into detail.

Figure 7 shows the spectra of Ti-ethyl and Al-monoethyl before (upper line) and after complex formation (lower line) at a temperature of  $220^\circ\text{K}$ . The two signals essential for the following points are (upper line) the Cp signal at 115.5 ppm and the Ti- $\text{CH}_2$  signal at 64.5 ppm relative to TMS. The results after complex formation at low temperatures are (lower line):

(i) All signals (excepting Ti- $\text{CH}_3$ ) are shifted downfield (for instance, Ti- $\text{CH}_2$  from 64.5 ppm to 84.6 ppm at an Al/Ti ratio of 2); hence, the shielding of the C nuclei is less in the complex or, in other words, the electronic density at the Ti center is lower after complex formation. This means that there is no electron back-donation of the AlEt group.

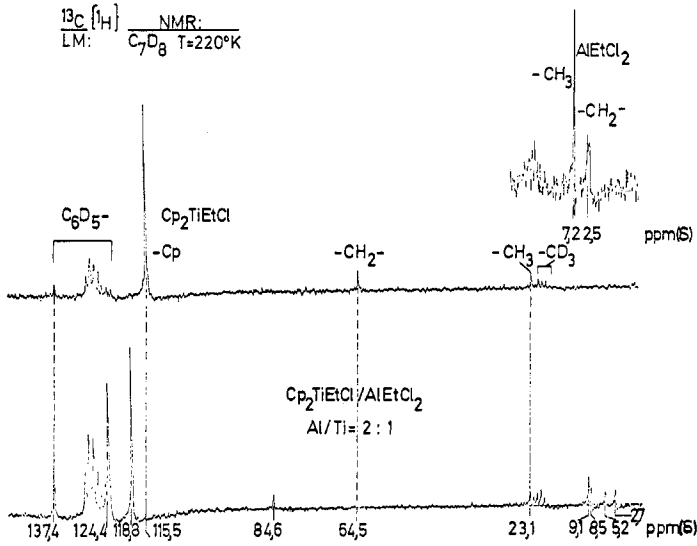


Fig. 7.  $^{13}\text{C}$ -NMR spectra of  $\text{Cp}_2\text{TiEtCl}$  and  $\text{AlEtCl}_2$  before (upper line) and after (lower line) complex formation in octadeuterotoluene at a temperature of  $220^\circ\text{K}$ . Ratio  $\text{Al/Ti} = 2$ .

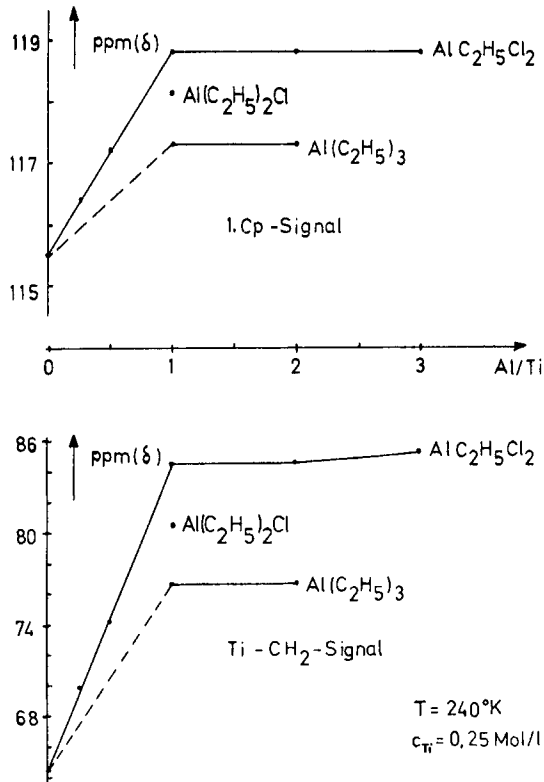


Fig. 8. Al isotherm of the primary complex in the systems  $\text{Cp}_2\text{TiEtCl}/\text{AlEt}_n\text{Cl}_m$  determined by  $^{13}\text{C}$ -NMR spectroscopy.  $[\text{Cp}_2\text{Ti-ethyl-Cl}] = 0.25 \text{ mole/l}$ ;  $T = 240^\circ\text{K}$ .



TABLE I  
Kinetic and Thermodynamic Data of the Primary Complex

Primary complex dissociation:

$$E_A: 6.0 \pm 1.5 \text{ (kcal/mole)}$$

$$k_0 \text{ (sec}^{-1}\text{): } 4.3 \times 10^9 < k_0 < 10^{13}$$

$$\Delta H^\ddagger \text{ (kcal/mole): } 4.0 < \Delta H^\ddagger < 6.9$$

$$\Delta S^\ddagger \text{ (e.u.): } -16 < \Delta S^\ddagger < -0.6$$

$$k_{\text{diss. } 220^\circ\text{K}} \text{ (sec}^{-1}\text{): } 1.4 \times 10^5 < k_{\text{diss.}} < 5.3 \times 10^5$$

$$k_{\text{diss. } 283^\circ\text{K}} \text{ (sec}^{-1}\text{): } 1.4 \times 10^6 < k_{\text{diss.}} < 2.2 \times 10^7$$

Primary complex formation:

$$k_{\text{for. } 220^\circ\text{K}} \text{ (l./mole}\cdot\text{sec): } 1.4 \times 10^9 < k_{\text{for.}} < 5.3 \times 10^9$$

$$k_{\text{for. } 283^\circ\text{K}} \text{ (l./mole}\cdot\text{sec): } 1.4 \times 10^{10} < k_{\text{for.}} < 2.2 \times 10^{11}$$

(ii) There are two Cp signals: the first (at 118 ppm) is an averaged signal due to the primary complex formation (see below). The second (at 124 ppm) shifts downfield continuously with rising Al concentration and with decreasing temperature. It is likewise an averaged Cp signal but due to the compound

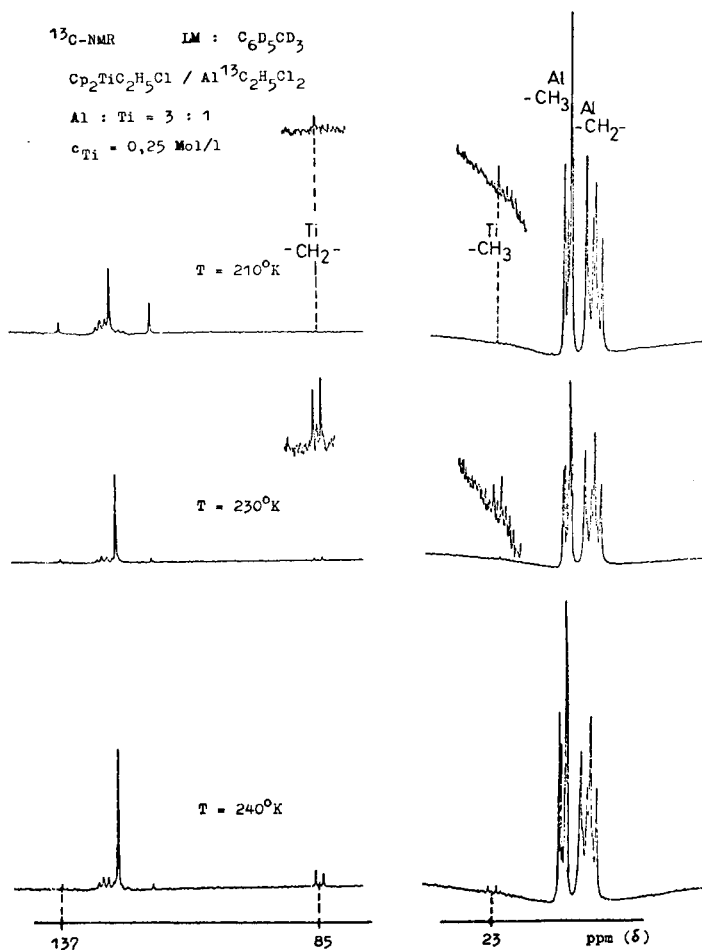


Fig. 9.  $^{13}\text{C-NMR}$  spectrum of a mixture of  $\text{Cp}_2\text{TiEtCl/AlEtCl}_2$  in  $\text{C}_6\text{D}_5\text{CD}_3$  with 1,2- $^{13}\text{C}$ -enriched Al-alkyl. Ratio Al/Ti = 3;  $[\text{Cp}_2\text{TiEtCl}] = 0.25 \text{ mole/l}$ .



Fig. 10.  $^{13}\text{C}$ -NMR spectrum of a mixture of  $\text{Cp}_2\text{TiEtCl}/\text{AlEt}_2\text{Cl}$  in  $\text{C}_6\text{D}_5\text{CD}_3$  with 1,2- $^{13}\text{C}$ -enriched Al-alkyl. Ratio Al/Ti = 1;  $[\text{Cp}_2\text{TiEtCl}] = 0.5$  mole/l.

$\text{Cp}_2\text{TiCl}_2$ , which is involved in a further parallel equilibria sequence (paper in preparation).  $\text{Cp}_2\text{TiCl}_2$  originates from  $\text{Cp}_2\text{TiEtCl}$  by a dealkylation reaction through the aluminum component, particularly if in a surplus.

We pursue the shift of the Ti- $\text{CH}_2$  and the first Cp signal (at 118 ppm) in dependence on the ratio Al/Ti. The result is plotted in Figure 8; it is the Al isotherm of the *primary complex*, for the first time measurable. The diagram proves the 1:1 Al/Ti stoichiometry of the primary complex (see also reaction scheme as above) which was postulated first by Breslow and Newburg<sup>6</sup> in the system  $\text{Cp}_2\text{TiCl}_2/\text{AlEt}_2\text{Cl}$  by means of UV spectroscopic investigations.

The comparison of the experimental *chemical shift* of the averaged Ti- $\text{CH}_2$  signal in Figure 8 with that as a function of  $K$  computed led here to a value of the equilibrium constant of the primary complex formation, that is,

$$5 \times 10^3 \leq K_1 \leq 5 \times 10^4 \quad (\text{at } 240^\circ\text{K})$$

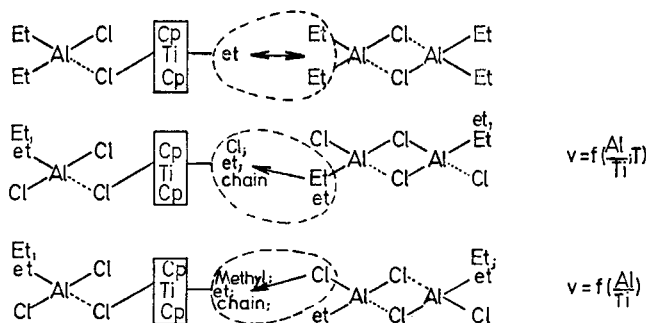


Fig. 11. Representation of reactions in the systems  $\text{Cp}_2\text{TiRCl}/\text{AlEt}_n\text{Cl}_m$ ; et:  $^{12}\text{CH}_2$ -,  $^{12}\text{CH}_3$ , normal alkyl; Et:  $^{13}\text{CH}_2$ -,  $^{13}\text{CH}_3$ , enriched alkyl.

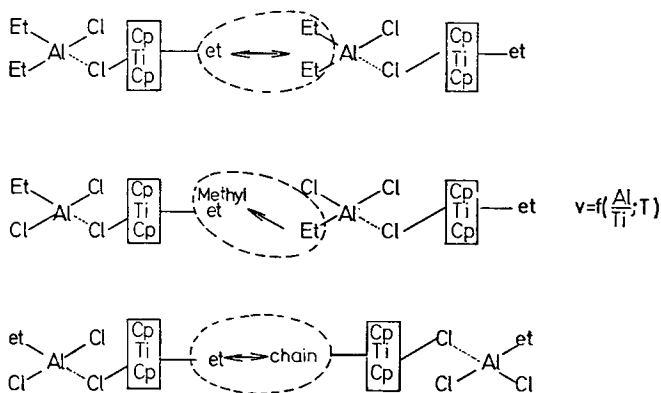


Fig. 12. Same as Fig. 11 (see text).

which is in agreement with the above kinetically deduced value. This value, i.e., also the location of the primary complex equilibrium, seems, according Figure 8, to be true for the three different Al components.

Looking at the point  $\text{Al/Ti} = 0.5$  in Figure 8, we have here complexed Ti and uncomplexed Ti in a ratio of 1:1, and the NMR  $\text{Ti-CH}_2$  signal is again the averaged signal of the rapid exchange process between the two positions Ti free in solution and Ti in complex. Pursuing the increasing line width of this averaged  $\text{Ti-CH}_2$  signal with decreasing temperature, we could calculate from the comparison of computer-simulated and experimental signal shapes exactly the *lifetime of the primary complex* and thus also rate constants. The result of this quantitative analysis is summarized in Table I.

In Table I it is to be noted that the second-order rate constant for the primary complex formation is (near room temperature) in the order of magnitude  $10^{10}$  to  $10^{11}$ . So we have a diffusion (i.e., physically) controlled reaction, that means, too, a collision frequency dependent reaction for this part of the reactions of soluble Ziegler catalysts.

The following two spectra demonstrate in another way insight into dynamic detail. We synthesized to about 50%  $1,2\text{-}^{13}\text{C}$ -enriched Al-alkyl. Looking at the signals at the right-hand side in Figure 9, one can see now triplets in the position of the  $\text{Al-CH}_2$  and  $\text{Al-CH}_3$  signals. This pseudotriplet structure is caused by  $^{13}\text{C}\text{-}^{13}\text{C}$  coupling, which generates an AB system; but near the centers of these doublets are the monosignals of only one  $^{13}\text{C}$ - or two  $^{13}\text{C}$ -enriched ethyl groups.

As soon as (in dependence on temperature) this "triplet structure" is appearing in the position of the  $\text{Ti-CH}_2$  and  $\text{Ti-CH}_3$  group, the replacement of the Ti-ethyl group through the Al-ethyl is directly indicated. This replacement occurs at an  $\text{Al/Ti}$  ratio = 3 and at a temperature of about  $230^\circ\text{K}$ , as visible in the middle spectrum. The effect is sufficient to be discerned by means of the enlargement. Figure 10 demonstrates this effect with Al-diethyl: now this alkyl transfer already occurs at  $210^\circ\text{K}$ . By means of these  $^{13}\text{C}$  enrichments, it was possible to detect many exchange reactions; these and others are systematized in the subsequent two schemes, which, however, are to be regarded as a first attempt only.

Thus, Figure 11 contains the processes between complexes and dimeric Al-alkyl (if in a surplus). (In Figs. 11 and 12, "et" means normal alkyl and "Et"

means 50% 1,2-<sup>13</sup>C-enriched Al-alkyl.) One of the things the middle line shows is also the transfer of a chain; in the lower line, we recognize a termination reaction which leads to the above-mentioned Cp<sub>2</sub>TiCl<sub>2</sub>.

In a similar way, Figure 12 shows the processes between two complexes; the reaction between two Ti centers (lower line) is to be emphasized.

At this point, we should briefly return to the inquiry into the structure of the polymerization active species. Realizing these numerous exchange reactions and realizing, furthermore, the great number of transition states possible as a consequence, the conclusion can be reached that many dynamic distorted configurations are possible which may possess the ability to insert ethylene.

The authors are indebted to DFG for supporting these investigations. They also thank Prof. Dr.Dr.h.c.F. Patat cordially for his permanent and supporting interest; this paper is dedicated to him in honor of his 70th birthday.

### References

1. W. Zoller, Dissertation TU München, 1974.
2. K. Meyer, K. H. Reichert, *Angew. Makromol. Chem.*, **12**, 175 (1970).
3. K. H. Reichert, *Angew. Makromol. Chem.*, **13**, 177 (1970).
4. G. Fink, *Amer. Chem. Soc., Polym. Div., Polym. Prepr.*, **13** (1), 443 (1972).
5. D. Schnell and G. Fink, *Angew. Makromol. Chem.*, **39**, 131 (1974).
6. D. S. Breslow and N. R. Newburg, *J. Amer. Chem. Soc.*, **81**, 81 (1959).

Received December 3, 1975